Journal of Zhejiang University-SCIENCE B (Biomedicine & Biotechnology)
ISSN 1673-1581 (Print); ISSN 1862-1783 (Online)
www.zju.edu.cn/jzus; www.springerlink.com
E-mail: jzus@zju.edu.cn

Derived vascular endothelial cells induced by mucoepidermoid carcinoma cells: 3-dimensional collagen matrix model*

Sen YANG[†§1,2], Li-juan GUO[§1], Qing-hong GAO[2], Ming XUAN[2], Ke TAN[3], Qiang ZHANG[3], Yu-ming WEN[2], Chang-mei WANG[2], Xiu-fa TANG[†‡2], Xiao-yi WANG[†‡2]

([1]*State Key Laboratory of Oral Diseases, Sichuan University, Chengdu 610041, China*)

([2]*Department of Head and Neck Tumor Surgery, West China College of Stomatology, Sichuan University, Chengdu 610041, China*)

([3]*Department of Health Statistics, West China College of Public Health, Sichuan University, Chengdu 610041, China*)

[†]E-mail: ys13880435413@163.com; tangxf1963@163.com; wxyz711@yahoo.com.cn

Received Dec. 27, 2009; Revision accepted Apr. 16, 2010; Crosschecked Sept. 7, 2010

Abstract: Mucoepidermoid carcinoma undergoes uniquely vigorous angiogenic and neovascularization processes, possibly due to proliferation of vascular endothelial cells (ECs) induced by mucoepidermoid carcinoma cells (MCCs) in their three-dimensional (3D) microenvironment. To date, no studies have dealt with tumor cells and vascular ECs from the same origin of mucoepidermoid carcinoma using the in vitro 3D microenvironment model. In this context, the current research aims to observe neovascularization with mucoepidermoid carcinoma microvascular ECs (MCMECs) conditioned by the microenvironment in the 3D collagen matrix model. We observed the growth of MCMECs purified by immunomagnetic beads and induced by MCCs, and characteristics of tubule-like structures (TLSs) formed by induced MCMECs or non-induced MCMECs. The assessment parameters involved the growth curve, the length, the outer and inner diameters, and the wall thickness of the TLSs, and the cell cycle. Results showed that MCCs induced formation of the TLSs in the 3D collagen matrix model. A statistically significant difference was noted regarding the count of TLSs between the control group and the induction group on the 4th day of culture (t=5.00, P=0.001). The outer and inner diameters (t_1=5.549, P_1=0.000; t_2=10.663, P_2=0.000) and lengths (t=18.035, P=0.000) of the TLSs in the induction group were statistically significant larger than those in the control group. The TLSs were formed at the earlier time in the induction group compared with the control group. It is concluded that MCCs promote growth and migration of MCMECs, and formation of the TLSs. The 3D collagen matrix model with MCMECs induced by MCCs in the current research may be a favorable choice for research on pro-angiogenic factors in progression of mucoepidermoid carcinoma.

Key words: Mucoepidermoid carcinoma, Vascular endothelial cells, 3-dimensional collagen matrix model
doi:10.1631/jzus.B0900404 **Document code:** A **CLC number:** Q37

1 Introduction

Containing squamous cells, mucus-secreting cells, and "intermediate" cells, mucoepidermoid carcinoma is regarded as one of the most common malignant primary tumors of maxillofacial salivary glands in both children and adults (Waldron *et al*., 1988; Lopes *et al*., 1999; Vargas *et al*., 2002). According to the revised WHO (2005)'s classification of tumors (Barnes *et al*., 2005), mucoepidermoid carcinoma is categorized into the well differentiated (low malignancy), moderately differentiated (moderate malignancy), and low differentiated (high malignancy) types in light of cell differentiation levels, biological features, and the proportion of mucus-secreting cells. The prognosis of mucoepidermoid carcinoma varies due to the different invasion capabilities of the three different types. The low malignancy mucoepidermoid

‡ Corresponding authors
§ The two authors contributed equally to this work
* Project (No. 0040305401042) supported by the National Natural Science Foundation of China

carcinoma grows slowly, resulting in both low regional and distant metastasis rates, while the moderately and highly malignant types spread rapidly with high regional and distant metastasis rates, leading to a poor prognosis. Mucoepidermoid carcinoma undergoes uniquely vigorous angiogenic and neovascularization processes, possibly due to proliferation of vascular endothelial cells (ECs) induced by tumor cells in the three-dimensional (3D) microenvironment of mucoepidermoid carcinoma (Yang *et al*., 2008). Tumor angiogenesis proceeds with evident heterogeneity, implying that tumor vascular ECs may be induced by tumor cells in the 3D microenvironment (Bian *et al*., 2004). To date, no studies have dealt with tumor cells and vascular ECs from the same origin of mucoepidermoid carcinoma using the in vitro 3D microenvironment model. In this context, the current research aims to observe neovascularization with mucoepidermoid carcinoma microvascular ECs (MCMECs) conditioned by the microenvironment in the 3D collagen matrix model.

2 Materials and methods

2.1 Mucoepidermoid carcinoma samples

Fresh mucoepidermoid carcinoma samples were obtained from the Department of Head and Neck Tumor Surgery, West China Hospital of Stomatology affiliated to Sichuan University, Chengdu, China. According to the revised WHO (2005)'s classification of tumors, the samples were identified as moderately differentiated mucoepidermoid carcinoma (originating from the soft palate) through pathology examination of conventional tissue sections with hematoxylin and eosin (HE) staining (Fig. 1). The post-surgery mucoepidermoid carcinoma tissues were rapidly transferred to Roswell Park Memorial Institute medium (RPMI-1640) containing 10% (v/v) fetal bovine serum (FBS) (HyClone, Logan, Utah, USA) precooled at 4 °C. Written informed consent was obtained from all patients/family to include their data in this study, which was approved by the ethics committee of West China College of Stomatology, Sichuan University, China.

2.2 Main reagents

Mouse anti-human cytokeratin monoclonal antibody, mouse anti-human vimentin antibody, mouse anti-human CD31 monoclonal antibody, mouse anti-human factor VIII related antigen monoclonal antibody, mouse anti-human CD34 monoclonal antibody, streptavidin peroxidase (SP) immunohistochemistry kit, and chromogenic agents were purchased from Sigma-Aldrich China Inc., Shanghai, China. RPMI-1640 complete medium, FBS, medium 131 supplemented with microvascular growth supplement (M131-MVGS), type IV collagenase, trypsin, cell dissociation buffer (CDB), and penicillin/streptomycin solution were purchased from R&D Systems China Inc., Shanghai, China. The immunomagnetic beads and Dynal magnetic particle concentrator (MPC) were purchased from Invitrogen Corp., Carlsbad, California, USA.

2.3 Isolation, purification, and culture of mucoepidermoid carcinoma cells (MCCs)

On a laminar flow clean workbench, mucoepidermoid carcinoma samples, pretreated with 10^5 U/L penicillin and 0.1 g/L streptomycin, were lightly rinsed three times with RPMI-1640 complete medium containing 10% FBS under sterile conditions. Mucoepidermoid carcinoma tissues were cut with sterile eye scissors into pieces of about 2 mm^3 that were placed in culture bottles for dispersion culture. A total of 2 ml RPMI-1640 complete medium was added after the culture bottles were slowly inverted. After 4 h, the bottles were turned to the normal position and a small volume of RPMI-1640 complete medium was added for additional culture. Characteristics of crawling cells and cell growth were visualized under the inverted microscope. RPMI-1640 complete medium was changed routinely until the cells reached 70%–80% confluency. The cells were digested with 0.25% (w/v) trypsin and adhered to the inner surface of culture bottles. The suspension was removed from the culture bottles 2 h later. The digestion procedure was repeated every 3 to 4 d before routine culture. After successful primary culture, MCCs and fibroblasts grew heterogeneously in patches. The two types of cells were separated gradually after the adherence separation method was repeated, regarding different characteristics of wall adherence.

2.4 Detection of cell markers for MCMECs with the immunohistochemistry assay

Fresh mucoepidermoid carcinoma samples were

fixed in 4% (w/v) paraformaldehyde for 30 min. Following conventional embedding procedures, they were sectioned sequentially at 4 μm. Specific expression of CD31 in MCMECs was detected with the SP immunohistochemistry assay as per the manufacturer's instructions. The identical volume of antibody dilution in place of the primary antibody was used as the negative control, whereas positive sections from the manufacturer were the positive controls.

2.5 Purification of MCMECs with immunomagnetic beads

Firstly, the immunomagnetic beads were completely resuspended. A total of 500 μl of immunomagnetic beads were shifted into test tube and rinsed as per the manufacture's instructions. Immunomagnetic beads were mixed with rat anti-mouse CD31 monoclonal antibody and were placed on the rocking bed at 4 ℃ overnight. Anti-CD31-coated immunomagnetic beads were rinsed three times with RPMI-1640 complete medium and were resuspended in 2-ml complete medium prior to storage at 4 ℃ for future use. Neovascularized tissues in the invasive periphery of mucoepidermoid carcinoma were incised and treated with 10^5 U/L penicillin and 0.1 g/L streptomycin. After being rinsed with RPMI-1640 complete medium, they were cut into pieces of 2 cm^3 under sterile conditions. The pieces were rinsed with RPMI-1640 complete medium and centrifuged at 210×*g* for 1 min. Then they were placed in 0.1% type IV collagenase (prepared with serum-free RPMI-1640 medium) for incubation at 37 °C for 1 h with constant horizontal shaking. Undigested tissues were retained with sterile 100-mesh steel wire cloth and transferred into four centrifuge tubes of 50 ml. A total of 40 ml precooled FBS was added into each test tube before centrifugation at 1000 r/min for 8 min. Enzyme-free cell dissociation buffer (CDB) was added for incubation for 5 min to obtain the suspension. The suspension was filtered through the 200-mesh, 300-mesh, and 400-mesh steel wire cloths, consecutively, following which they were rinsed twice with precooled RPMI-1640 complete medium. After centrifugation at 1000 r/min for 8 min, the cells were collected from the suspension and quantified. The collected cells were incubated with anti-CD31 coated immunomagnetic beads at 4 ℃ for 30 min, shaking constantly every 5 min for homogenization. The immunomagnetic beads were collected using magnetic separator (Dynal MPC, Oslo, Norway) for 2 min. The supernatants (with cells unbound to immunomagnetic beads) were removed and placed in sterile test tubes for another round of separation of immunomagnetic beads. The cells bound to the immunomagnetic beads were rinsed with the precooled RPMI-1640 complete medium for eight times until no unbound cells were visualized under the microscope, and cultured in M131-MVGS medium at 37 °C. The culture medium was changed after 24 h, and then every 48 to 72 h. The cell morphology was observed under the inverted phase contrast microscope.

2.6 Identification of MCCs and MCMECs

MCCs in primary culture and MCMECs purified with anti-CD31 immunomagnetic beads were adjusted to a density of 2×10^4 cells/ml. They were seeded on cover slides submerged in the wells of 6-well plates with 2 ml/well. When cells grew to 60%–80% of the area of the cover slides, the cover slides were removed and were rinsed with FBS twice. The slides were fixed in 4% paraformaldehyde for 30 min and dried for future use. The MCCs were identified using alcian blue staining and the SP immunohistochemistry assay (with mouse anti-human cytokeratin monoclonal antibody and mouse anti-human vimentin monoclonal antibody), while the MCMECs were detected with the mouse anti-human CD31 monoclonal antibody, mouse anti-human factor VIII related antigen monoclonal antibody, and mouse anti-human CD34 monoclonal antibody. The antibodies were diluted at a ratio of 1:100. The antibody dilution solution in place of the primary antibody was used as the negative control, whereas positive sections from the manufacturer were the positive controls. CD31 and CD34 positive cells had a buffy membrane, while other types of positive cells had a buffy cytoplasm (regarding other antibodies).

2.7 Preparation of rat tail collagen

Two Wistar rats weighing around 250 g (purchased from the West China Animal Experiment Center, Sichuan University, Chengdu, China) were used in this experiment. After the tail epidermis was removed under sterile conditions, the tail tendon was disconnected and minced into pieces. The pieces were

placed in 0.1% (v/v) sterile acetic acid solution at 4 °C and shaken for 48 h. The mixture was separated and centrifuged at 4000 r/min for 30 min at 4 °C. The supernatants were removed and diluted to the original working solution at a ratio of 1:3 (acetic acid added for the dilution purpose). The original collagen working solution, FBS, 10× RPMI-1640 complete medium, and $NaHCO_3$ at a ratio of 7:1:1:1 (v/v) were molded in the ice bath.

2.8 3D collagen matrix model and grouping

A total of 0.5 ml identified MCMECs, following purification with immunomagnetic beads, were seeded at 2×10^4 cells/ml in a 24-well plate with tail collagen medium. The plate was placed for incubation at 37 °C with 5% CO_2 under saturated humidity. The culture medium was changed every 3 d. MCMECs were observed and recorded once a day. Two experiment groups were designated: 3D control group, collagen medium plus serum-free RPMI-1640 medium; and 3D induction group, collagen medium plus induction solution. The induction solution was prepared with serum-free RPMI-1640 medium (1/3) plus supernatants (2/3) from culture of purified MCCs (from primary culture) for 48 h.

2.9 Observation of tubule-like structures (TLSs)

The TLSs were counted at an interval of 2 d starting from 2 d after culture in the two experiment groups. The TLSs in six wells for each group were counted repeatedly three times and the average count of the TLSs for each well was tabulated into the growth curve. MCMECs crawled on cover slides and were stained with HE. The ultrastructure of the TLS was randomly analyzed with the MD-20 Image Analysis System with Synchronized Predeployment and Operational Tracker (SPOT) Version 4.0.8 software (Leica, Solms, German).

2.10 Detection by flow cytometry

MCMECs in the two experiment groups were cultured for 2 d, followed by trypsin digestion and FBS rinsing twice. They were filtered through the 250-mesh steel wire cloth. The digestion of MCMECs was terminated by RPMI-1640 complete medium. After centrifugation, MCMECs were fixed with 70% (v/v) ethanol precooled at 4 °C and stained with 25 μg/ml propidium iodide (PI). The cell cycle of MCMECs was detected with the EPICS Elite ESP flow cytometer (Beckman Coulter, Los Angeles, California, USA).

2.11 Statistical analysis

All analyses were carried out using Statistical Package for the Social Science (SPSS) Version 13.0. Continual variables were expressed as mean±standard deviation (SD). Student *t*-test was used for comparison between two groups. A statistically significant difference was considered if $P<0.05$.

3 Results

3.1 Morphology of MCCs and identification

On the 5th day of culture of mucoepidermoid carcinoma tissues, the cell halo was visualized under the inverted microscope, around some mucoepidermoid carcinoma tissues. Like typical epithelial cells, MCCs grew in cobblestone patterns. With time, cell colonies expanded and some MCCs demonstrated dispersed growth. At the same time, bundle-shaped or whirlpool-shaped fibroblasts were visualized. In primary culture, the culture medium was changed every 3 d. The first cell passage started on the 18th day of culture, followed by other passages every 3 to 4 d. In light of different characteristics of wall adherence between MCCs and fibroblasts, MCCs were gradually separated from fibroblasts after the adherence separation method was repeated. Most purified MCCs were different-sized polygonal epithelial cells with a giant, round cell nucleus and a high karyoplasmic ratio. Some MCCs were oval epithelial cells, but multinucleated giant cells or megakaryocytes were rarely visualized. Purified MCCs at the 15th passage were selected and stained with HE. When 1000 MCCs were considered, polygonal epithelial cells, oval epithelial cells, and giant cells accounted for 98%, 1.2%, and 0.8%, respectively. With immunohistochemical staining for cytokeratin, cytoplasm and membrane of nearly all MCCs showed apparent buffy granules. With immunohistochemical staining for vimentin, almost all MCCs were negative. After alcian blue staining, only 15% MCCs were stained blue in the cytoplasm (Fig. 1).

3.2 Detection of MCMEC marker

CD31 was specifically expressed in vascular ECs in the mucoepidermoid carcinoma, though CD31-positive microvessels were distributed unevenly. "Hot-spot areas" existed mainly in the invasive periphery of mucoepidermoid carcinoma (Fig. 2).

3.3 Morphology of MCMECs purified with immunomagnetic beads and identification

At 6 h after MCMECs purified with immunomagnetic beads were inoculated, they adhered to the inner surface of culture bottles. At 48 h, the MCMECs grew confluent in a single cobblestone-shaped flat layer. Under the microscope, the membrane of MCMECs was typically buffy using the immunohistochemistry assay for CD34. With detection of factor VIII related antigen, cytoplasm of MCMECs was stained buffy under the microscope (Fig. 3).

3.4 Count of TLSs in 3D collagen matrix model

After MCMECs were purified and identified with immunomagnetic beads, they were cultured for 14 d in the 3D collagen matrix model. Counts of the TLSs were recorded in Table 1.

3.5 Parameters of TLSs

The TLSs were thick and long in the induction group, while they were thin and short in the control group (Fig. 4). The length, outer and inner diameters, and wall thickness of the TLSs formed by MCMECs were assessed. Assessment results are summarized in Table 2.

3.6 Cell cycle assay

While the count of MCMECs increased in both the S and G_2/M phases, it decreased with shortened cell cycle in the G_0/G_1 phase in the induction group, as compared with the control group (Fig. 5).

4 Discussion

Tumor angiogenesis facilitates growth, invasion, and metastasis of tumor. Folkman (1971) put forward the concept that tumor growth necessitates neovascularization. It was considered that the tumor is living on nutrients and oxygen diffusing to it if the diameter of the solid tumor is less than 1 or 2 mm, while neovessels are required to guarantee the supply of nutrients if the diameter is over 2 mm. Tumor tissues degenerate when no neovessels grow in, but expand with a high potential of invasion and metastasis immediately following neovascularization, this being regarded as "the balance for the angiogenesis switch" by Folkman (1971; 1996). Tumors not only obtain nutrients and exchange metabolites and air through neovessels in tumor tissues, but also transit numerous cancer cells to other areas by metastasis and

Table 1 Counts of TLSs formed by MCMECs at different culture time in 3D collagen matrix model

Group	Count of TLSs						
	2 d	4 d	6 d	8 d	10 d	12 d	14 d
Control	0.33±0.52	1.33±0.52	3.33±0.82	4.33±0.82	6.50±1.05	8.33±1.17	10.80±1.16
Induction	0.83±0.41	3.00±0.63	7.83±0.98	12.00±1.41	14.80±1.17	17.10±0.98	20.60±1.21
t	1.86	5.00	8.63	11.50	13.00	13.36	14.31
P	0.092	0.001	0.000	0.000	0.000	0.000	0.000

After MCMECs were purified, they were cultured for 14 d in the 3D collagen matrix model. Data are expressed as mean±SD (n=6). A statistically significant difference was noted regarding the counts of TLSs between the control group and the induction group after the 4th day of culture (t=5.00, P=0.001)

Table 2 Parameters of TLSs formed by MCMECs

Group	Outer diameter (μm)	Inner diameter (μm)	Wall thickness (μm)	Length (μm)
Control	448.47±25.30	211.19±8.38	194.85±7.40	451.13±29.40
Induction	551.01±37.05	338.23±27.96	189.21±8.84	756.47±29.25
t	5.549	10.663	1.200	18.035
P	0.000	0.000	0.258	0.000

Several parameters of the TLSs formed by MCMECs were detected. Data are expressed as mean±SD (n=6). The outer and inner diameters (t_1=5.549, P_1=0.000; t_2=10.663, P_2=0.000) and length (t=18.035, P=0.000) of the TLSs in the induction group were larger than those in the control group, and TLSs were formed at the earlier time in the induction group

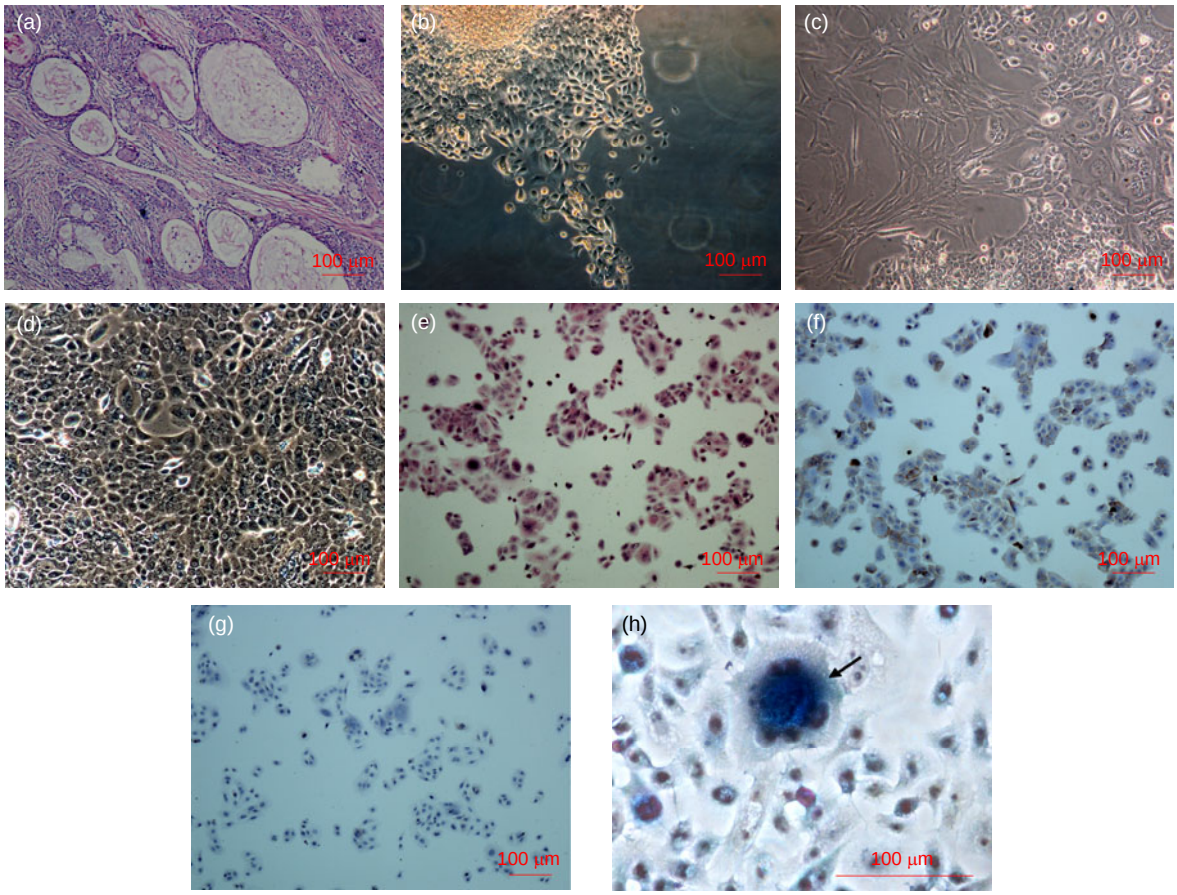

Fig. 1 Isolation, purification, culture, and identification of MCCs

(a) Tissue specimens were obtained from the soft palate. HE staining revealed that there were mucus-secreting cells, epidermal like cells, and intermediate cells; (b) After the tissue specimen was cultured for 5 d, it was found, under the inverted microscope, that cell halo grew around some mucoepidermoid carcinoma tissues. The MCCs grew in typical cobblestone patterns; (c) After the tissue specimen was cultured for 10 d, colonies of MCCs gradually expanded. Among the MCCs, some fibroblasts were bundle-shaped or whirlpool-shaped; (d) Most purified MCCs were different-sized polygonal epithelial cells with a giant cell nucleus and a high karyoplasmic ratio. Very few were oval epithelial cells; (e) HE staining for purified MCCs showed no spindle-shaped or fibroblast-like cells, but polygonal epithelial cells appeared in various colonies; (f) With immunohistochemical staining for cytokeratin, cytoplasm and membrane of nearly all MCCs showed buffy granules; (g) With immunohistochemical staining for vimentin, almost all cells were negatively stained; (h) Alcian blue staining showed obvious blue staining in mucus-secreting cells as indicated with the arrow

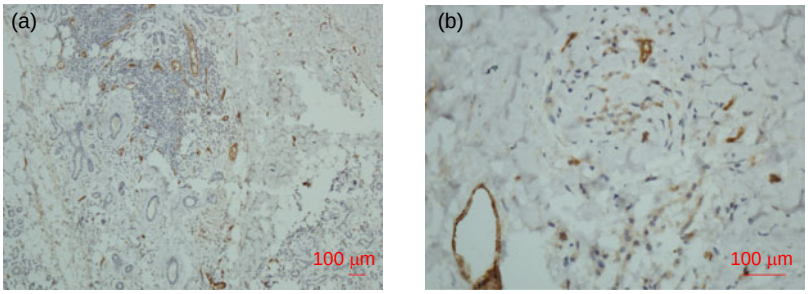

Fig. 2 Immunohistochemistry assay of MCMECs

(a) Capillary vascularization could be seen in tumor growth actively region; (b) CD31 was specifically expressed in vascular ECs in the invasive periphery of mucoepidermoid carcinoma where numerous neovascularized tissues concentrated

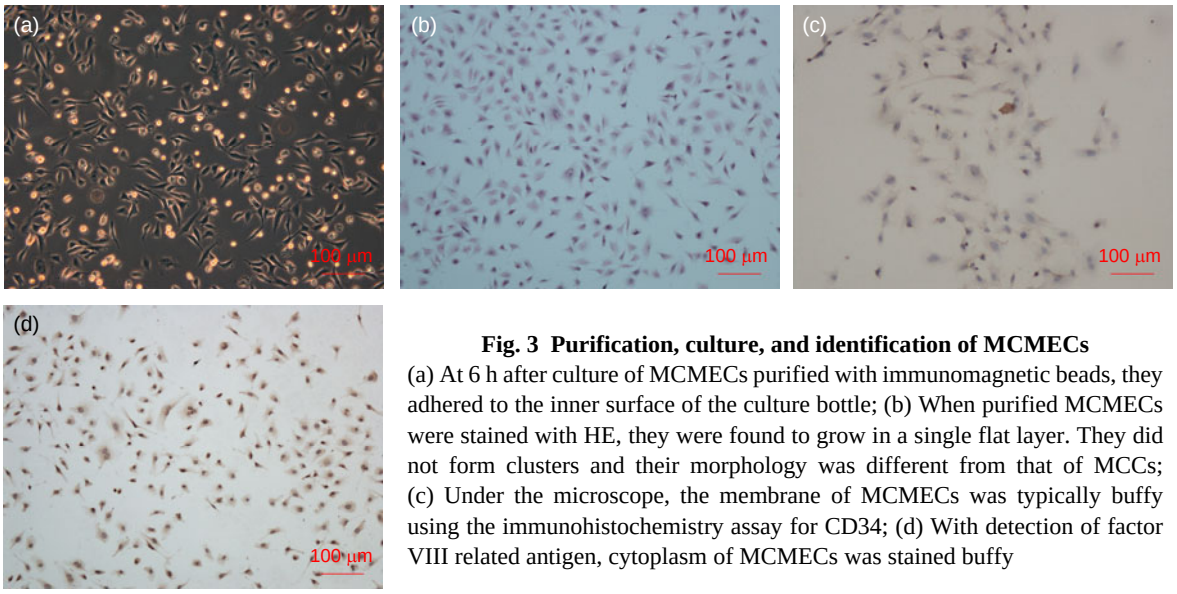

Fig. 3 Purification, culture, and identification of MCMECs

(a) At 6 h after culture of MCMECs purified with immunomagnetic beads, they adhered to the inner surface of the culture bottle; (b) When purified MCMECs were stained with HE, they were found to grow in a single flat layer. They did not form clusters and their morphology was different from that of MCCs; (c) Under the microscope, the membrane of MCMECs was typically buffy using the immunohistochemistry assay for CD34; (d) With detection of factor VIII related antigen, cytoplasm of MCMECs was stained buffy

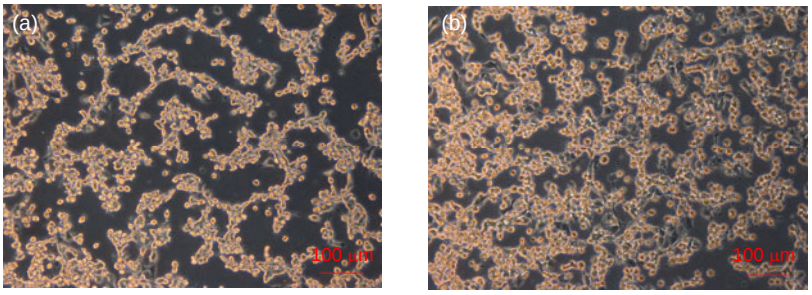

Fig. 4 Comparison of TLS parameters in the induction (a) and control (b) groups

The TLSs were thick and long in the induction group, while they were thin and short in the control group

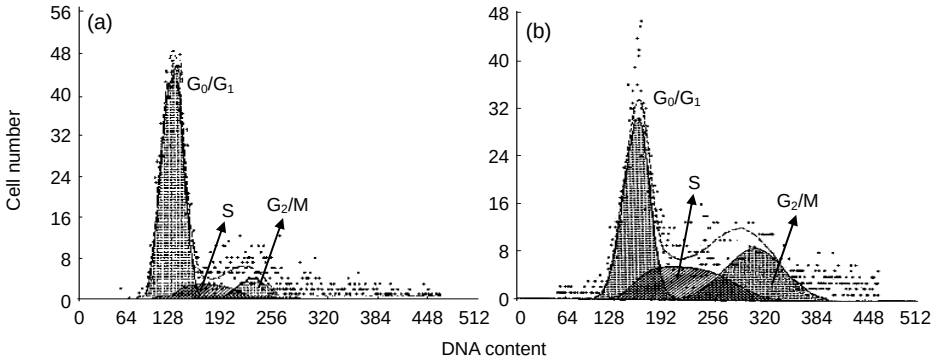

Fig. 5 Comparison of cell cycles in the control (a) and induction (b) groups

The count of MCMECs increased in both the S and G_2/M phases, but decreased in the G_0/G_1 phase in the induction group, as compared with the control group

invasion (Konerding *et al*., 1998; Bian, 2001; Shirakawa *et al*., 2002a; 2002b; Brat and van Meir, 2004). Some studies have indicated that activated ECs have an essential role in initiating the onset of tumor angiogenesis that is regulated by positive/negative regulation factors secreted by tumor (Hendrix *et al*., 2001; Hess *et al*., 2001; Zeng *et al*., 2005). The current research selected mucoepidermoid carcinoma supernatants as the induction agent for establishment of in vitro model of angiogenesis in mucoepidermoid

carcinoma. As tumor vascular ECs of different origins vary in structure and function (Bian *et al*., 2004; 2006; Lorincz *et al*., 2005), MCMECs are a desired option to establish an in vitro model of angiogenesis in mucoepidermoid carcinoma. However, the vascular ECs are scarce, and the isolation and purification processes are easily influenced by many factors. Recently, it has been revealed that many tumor vascular ECs specifically express CD31 (Parums *et al*., 1990; Kuzu *et al*., 1992; Miettinen *et al*., 1994; Hao *et al*., 2002). To effectively isolate MCMECs from the cell mixture, the current research used immunomagnetic beads to purify the limited amount of CD31-positive tumor vascular ECs derived from mucoepidermoid carcinoma. When CD31-positive tumor vascular ECs were detected for factor VIII related antigen and CD34, the results confirmed that both were strongly positively expressed. The in vitro model of angiogenesis in mucoepidermoid carcinoma was thus successfully constructed with MCMECs.

Tumor angiogenesis is so complex that well-constructed in vitro and in vivo models are required for in-depth research. As the internal environment is complex and changeable in in vivo model, the in vitro model demonstrates advantages in studying some signal transduction pathways. Before 1980s, in vitro studies on tumor angiogenesis of vascular ECs were limited on the two-dimensional (2D) culture and no 3D environment was available, so in vitro tumor neovascularization was inadequately assessed. The 3D culture of vascular ECs takes advantage of the characteristic that in vitro vascular ECs form TLSs under certain conditions, which highlights it as one of the best options to explore in vivo angiogenesis. The current research isolated and purified MCCs and MCMECs derived from the same tumor origin, in order to construct the in vitro 3D model that accurately simulates the 3D microenvironment in which MCCs induced adhesion, proliferation, and metastasis of MCMECs.

In the current research, MCMECs grew slowly in cobblestone patterns or formed scattered small and short TLSs in the 3D control group without induction of MCCs. However, in the induction group with supernatants of MCCs, MCMECs grew significantly faster and the TLSs were bigger and longer, which implied that replication of chromosomes in vascular ECs became faster. The flow cytometry assay found that the count of MCMECs increased in the G_2/M phase while decreasing in the G_0/G_1 phase, indicating that MCCs statistically significantly shortened the chromosome replication cycle and facilitated proliferation of MCMECs.

In the current in vitro model, vascular ECs formed pervasively long and large TLSs. They aligned in order, but barely formed complete vessel walls. This may result from lack of support from vascular smooth muscles. The model accurately simulates angiogenic and neovascularization processes in vivo, exhibiting interaction of various factors of these processes. It provides a methodology for in-depth understanding of the molecular mechanism of angiogenesis and possibly contributes to anti-angiogenesis therapy for mucoepidermoid carcinoma.

5 Acknowledgements

We thank Dr. Steven PAN (West China School of Public Health of Sichuan University, China) for his meticulous efforts in reviewing the paper. His innovative and critical suggestions and advice significantly contributed to the final version of the paper.

References

Barnes, L., Eveson, J.W., Reichart, P., Sidransky, D., 2005. World Health Organization Classification of Tumours: Pathology and Genetics of Head and Neck Tumours. IARC Press, Lyon, France, p.219-220.

Bian, X.W., 2001. Angiogenesis, therapeutic angiogenesis and antiangiogenesis. *Acta Acad. Med. Milit. Tert.*, **23**(3): 249-250 (in Chinese).

Bian, X.W., Chen, J.H., Jiang, X.F., Bai, J.S., Wang, Q.L., Zhang, X., 2004. Angiogenesis as an immunopharmacologic target in inflammation and cancer. *Int. Immunopharmacol.*, **4**(12):1537-1547. [doi:10.1016/j.intimp.2004.07.017]

Bian, X.W., Jiang, X.F., Chen, J.H., Bai, J.S., Dai, C., Wang, Q.L., Lu, J.Y., Zhao, W., Xin, R., Liu, M.Y., *et al*., 2006. Increased angiogenic capabilities of endothelial cells from microvessels of malignant human gliomas. *Int. Immunopharmacol.*, **6**(1):90-99. [doi:10.1016/j.intimp.2005.08.004]

Brat, D.J., van Meir, E.G., 2004. Vaso-occlusive and prothrombotic mechanisms associated with tumor hypoxia, necrosis, and accelerated growth in glioblastoma. *Lab. Invest.*, **84**(4):397-405. [doi:10.1038/labinvest.3700070]

Folkman, J., 1971. Tumor angiogenesis: therapeutic implications. *N. Engl. J. Med.*, **285**(21):1182-1186.

Folkman, J., 1996. Fighting cancer by attacking its blood supply. *Sci. Am.*, **275**(3):150-154. [doi:10.1038/scientificamerican0996-150]

Hao, X., Sun, B., Zhang, S., Zhao, X., 2002. Microarray study of vasculogenic mimicry in bi-directional differentiation malignant tumor. *Natl. Med. J. China*, **82**(19):1298-1302 (in Chinese).

Hendrix, M.J., Seftor, E.A., Meltzer, P.S., Gardner, L.M., Hess, A.R., Kirschmann, D.A., Schatteman, G.C., Seftor, R.E., 2001. Expression and functional significance of VE-cadherin in aggressive human melanoma cells: role in vasculogenic mimicry. *PNSA*, **98**(14):8018-8023. [doi:10.1073/pnas.131209798]

Hess, A.R., Seftor, E.A., Gardner, L.M., Carles-Kinch, K., Schneider, G.B., Seftor, R.E., Kinch, M.S., Hendrix, M.J., 2001. Molecular regulation of tumor cell vasculogenic mimicry by tyrosine phosphorylation: role of epithelial cell kinase (Eck/EphA2). *Cancer Res.*, **61**(8):3250-3255.

Konerding, M.A., Fait, E., Dimitropoulou, C., Malkusch, W., Ferri, C., Giavazzi, R., Coltrini, D., Presta, M., 1998. Impact of fibroblast growth factor-2 on tumor microvascular architecture: a tridimensional morphometric study. *Am. J. Pathol.*, **152**(6):1607-1616.

Kuzu, L., Bicknell, R., Harris, A.L., Jones, M., Gatter, K.C., Mason, D.Y., 1992. Heterogeneity of vascular endothelial cells with relevance to diagnosis of vascular tumours. *J. Clin. Pathol.*, **45**(2):143-148. [doi:10.1136/jcp.45.2.143]

Lopes, M.A., Kowalski, L.P., Santos, G.C., de Almeida, O.P., 1999. A clinicopathologic study of 196 intraoral minor salivary gland tumours. *J. Oral Pathol. Med.*, **28**(6):264-267. [doi:10.1016/S0278-2391(00)90075-2]

Lorincz, T., Toth, J., Szendroi, M., Timar, J., 2005. Microvascular density of breast cancer in bone metastasis: influence of therapy. *Anticancer Res.*, **25**(4):3075-3081.

Miettinen, M., Lindenmayer, A.E., Chaubal, A., 1994. Endothelial cell markers CD31, CD34, and BNH9 antibody to H- and Y-antigens-evaluation of their specificity and sensitivity in the diagnosis of vascular tumors and comparison with von Willebrand factor. *Mod. Pathol.*, **7**(1):82-90.

Parums, D.V., Cordell, J.L., Micklem, K., Heryet, A.R., Gatter, K.C., Mason, D.Y., 1990. JC70: a new monoclonal antibody that detects vascular endothelium associated antigen on routinely processed tissue sections. *J. Clin. Pathol.*, **43**(9):752-757. [doi:10.1136/jcp.43.9.752]

Shirakawa, K., Kobayashi, H., Heike, Y., Kawamoto, S., Brechbiel, M.W., Kasumi, F., Iwanaga, T., Konishi, F., Terada, M., Wakasugi, H., 2002a. Hemodynamics in vasculogenic mimicry and angiogenesis of inflammatory breast cancer xenograft. *Cancer Res.*, **62**(2):560-566.

Shirakawa, K., Wakasugi, H., Heike, Y., Watanabe, I., Yamada, S., Saito, K., Konishi, F., 2002b. Vasculogenic mimicry and pseudo-comedo formation in breast cancer. *Int. J. Cancer*, **99**(6):821-828. [doi:10.1002/ijc.10423]

Vargas, P.A., Gerhard, R., Araújo Filho, V.J., de Castro, I.V., 2002. Salivary gland tumors in a Brazilian population: a retrospective study of 124 cases. *Rev. Hosp. Clin. Fac. Med. Sao. Paulo.*, **57**(6):271-276.

Waldron, C.A., el-Mofty, S.K., Gnepp, D.R., 1988. Tumors of the intraoral minor salivary glands: a demographic and histologic study of 426 cases. *Oral Surg. Oral Med. Oral Pathol.*, **66**(3):323-333. [doi:10.1016/0030-4220(88)90240-X]

Yang, S., Wang, X.Y., Guo, L.J., Tang, X.F., Gao, Q.H., Xuan, M., Zhang, Q., Tan, K., Wen, Y.M., Wang, C.M., *et al.*, 2008. Correlation between the expression of thrombospondin-1 and neovascularization in mucoepidermoid carcinoma. *Chin. Med. J.*, **121**(19):1875-1881.

Zeng, Q., Li, S., Chepeha, D.B., Giordano, T.J., Li, J., Zhang, H., Polverini, P., Nor, J., Kitajewski, J., Wang, C., 2005. Crosstalk between tumor and endothelial cells promotes tumor angiogenesis by MAPK activation of Notch signaling. *Cancer Cell*, **8**(1):13-23. [doi:10.1016/j.ccr.2005.06.004]

2009 JCR of Thomson Reuters for *JZUS-B* and *JZUS-A*

ISI Web of Knowledge℠

Journal Citation Reports®

WELCOME | HELP | RETURN TO LIST | PREVIOUS JOURNAL | NEXT JOURNAL

2009 JCR Science Edition

Journal: Journal of Zhejiang University-SCIENCE B

Mark	Journal Title	ISSN	Total Cites	Impact Factor	5-Year Impact Factor	Immediacy Index	Citable Items	Cited Half-life	Citing Half-life
☐	J ZHEJIANG UNIV-SC B	1673-1581	619	1.041		0.156	128	3.1	7.5

Journal: Journal of Zhejiang University-SCIENCE A

Mark	Journal Title	ISSN	Total Cites	Impact Factor	5-Year Impact Factor	Immediacy Index	Citable Items	Cited Half-life	Citing Half-life
☐	J ZHEJIANG UNIV-SC A	1673-565X	322	0.301		0.066	213	3.0	6.8